Hemorrhagic Transformation in Patients With Large-artery Atherosclerotic Stroke Is Associated With Gut Microbiota and LPS-TLR4 Signaling Pathway

Qin Huang
Xiangya Hospital Central South University
Min-Ping Wei
Xiangya Hospital Central South University
Xian-Jing Feng
Xiangya Hospital Central South University
Fang Yu
Xiangya Hospital Central South University
Di Liao
Xiangya Hospital Central South University
Ze-Yu Liu
Xiangya Hospital Central South University
Yun-Fang Luo
Xiangya Hospital Central South University
Ting-Ting Zhao
Xiangya Hospital Central South University
Ru-Xin Tu
Xiangya Hospital Central South University
Qing Huang
Xiangya Hospital Central South University
Yun-Hai Liu
Xiangya Hospital Central South University
xia Jian (xjian1216@csu.edu.cn)
Xiangya Hospital Central South University

Research Article

Keywords: Gut microbiota, stroke, hemorrhagic transformation, lipopolysaccharide, inflammation

Posted Date: November 30th, 2021

DOI: https://doi.org/10.21203/rs.3.rs-1111188/v1

Abstract

Objective: Hemorrhagic transformation (HT) is a major complication of ischemic stroke that worsens outcomes and increases mortality. Disruption of gut microbiota is an important feature of stroke, and some special bacteria combined with bacterial metabolites may contribute to HT pathogenesis. we aimed to study the relationship between gut microbiota and HT of large-artery atherosclerotic stroke.

Methods: From May-2020 through September-2021, the blood and fecal samples in patients with acute first-ever ischemic stroke and not undergoing intravenous thrombolysis or endovascular were obtained on admission, and gut microbiota was assessed by 16s ribosomal ribonucleic acid (rRNA) sequence. Stroke that developed HT (n=15) were compared to those without HT (n=17) and healthy controls (n=16). We also examined the key components of lipopolysaccharide (LPS) pathway: LPS, LPS-binding protein (LBP), and solube CD14 (sCD14). The role of gut microbiota in HT was evaluated using experimental stroke model.

Results: We observed that bacterial diversity was decreased in both HT and non-HT group compared to the healthy controls. The patients of ischemic stroke that developed HT had differential composition of gut microbiota, in particular, an increase in the relative abundance and diversity of members belonging to the Enterobacteriaceae family. Plasma LPS and LBP levels were higher in HT group compared to non-HT group. The concentrations of LPS, LBP and sCD14 were associated with increased abundance of Enterobacteriaceae. In experimental study, the antibiotics treatment diminished HT-induced increase in the levels of LPS and LBP as well as upregulated expression of Toll-like receptor 4 (TLR4) and NF-κB in colon tissue. Transplant of microbiota from HT rats triggered higher level of LPS, LBP and sCD14 in plasma and increased expression of TLR4 and NF-κB in colon tissue.

Conclusion: Stroke patients who developed with HT exhibit an obvious change in gut microbiota and LPS-induced inflammatory response. This suggests that maintaining a balance of gut microbiota may be an important factor in preventing HT after stroke.

Background

Hemorrhagic transformation (HT) is one of the most serious complications in acute ischemic stroke, which can exacerbate ischemic injury of brain by promoting glial and neuronal cell death, resulting in worse stroke outcomes and increased mortality (1). As the potential severe adverse event of tissue plasminogen activator (tPA), which remains the gold standard treatment for stroke within 4.5 hours, HT limits the benefit from tPA treatment (2). However, identifying high risk of HT in ischemic stroke is challenging, and none reliable therapies is sufficient to reduce the risk of HT, especially post-thrombolysis in stroke (3, 4). Considering the intricate mechanisms underlying HT progression, identifying high risk of HT and developing effective new treatments for HT is an imperative challenge.

Lipopolysaccharide (LPS), which is expressed by many classes of commensal enteric bacteria, can be interacted with TLR4 on the cell surface, regulates NF-κB transcriptional activation of inflammatory

genes, including TNF-α,IL-6 and IL-1β. ultimately lead to the dysregulation of inflammatory responses (5). These cytokines play important roles in the development of stroke and are also implicated in the pathophysiology of ischemic lesions (6). According to an experimental study, metabolic endotoxemia promoted LPS-induced neuroinflammation and affect the outcome after stroke. LPS and E.coli (which belongs to the Enterobacteriaceae family) were localized in the peri-infarct area and is associated with activation of TLR4 signaling (7). In a clinic study about stroke patients, LPS-producing bacteria was significantly altered and the pathways about Lipopolysaccharide biosynthesis proteins was correspondingly changed (8). LPS-binding protein (LBP) facilitates the extraction of LPS monomers by receptor CD14 (presented in a circulating soluble form, sCD14), which in turn contributes to the interaction of LPS and TLR4 (9). sCD14 can bind to Escherichia coli (10) and activated in microglia/macrophages following human traumatic brain injury (11). Bacterial load in blood and lungs challenged by Escherichia coli in CD14-deficient mice was reduced (12, 13). Recently, LBP and sCD14 have been suggested as clinical markers of endotoxemia that better reflect plasma exposure to LPS in stroke (14), its comorbidities (15, 16) , and other neurological diseases (17). However, the association between the proxy biomarkers of gut dysbiosis and systemic low-grade inflammation (LPS, LPB, and sCD14) and HT pathophysiology remains unclear.

The link between the gut and brain, the so-called gut-brain axis, has recently gained increasing attention. Gut microbiota affected ischemic stroke progression through a strong inflammatory component (18). Normally, the host maintains homeostasis with its gut microbiota through immune supervision, nutrition supply and barrier system (19). Disturbance of this homeostasis increases stroke risk (20) and deteriorates outcomes (21). Stroke can rapidly disturb gut homeostasis as indicated by the significant gut dysbiosis observed in related animal experiments (22, 23) and various stroke cohort studies (24, 25). Moreover, the stroke-induced overgrowth of Enterobacteriaceae, in turn, accelerates systemic inflammation through LPS-TLR4 pathway and exacerbates brain infarction (26). Also, intestinal inflammation is associated with impairment of gut-brain vascular barrier and recruitment of inflammatory cells to distal organs, which is promoted by bacteria-derived LPS (27). In this context, we recently have shown in experimental study that the peripheral immune response in HT after ischemic stroke can be characterized by gut microbiota (28), thus implying a reciprocally relationship between dysbiosis and HT. Nevertheless, the bidirectional interaction between HT and gut microbiota remains largely unknown, especially in stroke patients with HT. In this study, we sought to determine whether differences in gut microbiota are present in HT and non-HT stroke patients. Such changed gut microbiota and associated pathways may be early markers of HT risk or therapeutic targets to reduce HT.

Materials And Methods

Study population

The patients who were admitted within 7 days of symptom onset and were consecutively enrolled between May 2020 and September 2021 in the department of Neurology of Xiangya Hospital of Central South University (Hunan, China) were retrospective screened for this study. We initially identified and

screened stroke patients with large-artery atherosclerosis classified by the Trial of Org 10172 in Acute Stroke Treatment (TOAST) criteria (29), while other determined or undetermined stroke etiologies were excluded (Fig. 1). The inclusion criteria of this study were as follows: aged ≥18 years; acute first-ever ischemic stroke; without undergoing intravenous thrombolysis or endovascular thrombectomy, and availability of MRI or CT for evaluating HT. Patients with advanced cancer, other internal of neurological diseases, diabetes (type 1 and 2), or gastrointestinal disease (including inflammatory bowel disease, celiac disease, intestinal surgery, chronic pancreatitis or other malabsorption disorder) in the past 3 months were excluded. Individuals were also excluded if they had received antibiotics or probiotics within the last 3 months. Attending neurologists assessed neurological status for each patient daily. Patients underwent baseline neuroimaging and follow-up imaging with MRI or CT within 7 days post-stroke. Finally, 16 target patients with HT and 17 matching patients with negative HT were recruited. A control group of 15 healthy subjects without inflammatory diseases or neurological disorders was also studied. Blood and fecal samples were collected at admission after the initial diagnosis. The study was approved by the Ethics Committee of Xiangya Hospital of Central South University and all participants provided written informed consent in accordance with the Declaration of Helsinki.

Clinical data collection and detection of HT

The baseline characteristics, vascular risk factors, acute stroke management, and other laboratory findings of the included patients were obtained by reviewing electronic medical records. Clinical stroke severity was assessed at admission using the National Institutes of Health Stroke Scale (NIHSS) (30). Study patients had a brain MRI or CT at hospital admission but had no evidence of hemorrhage. One or more follow-up brain images were performed in all patients according to an institutional stroke imaging protocol. Follow-up brain images were carried out at the time of any clinical worsening or at 5-7 days after admission. HT was detected on those follow-up brain images. CT-detected HT was defined as the part of increase density in an area of low attenuation (31). In MRI images, the combination of diffusion-weighted imaging (DWI), fluid-attenuation inversion recovery (FLAIR), T1-weighting and T2-weighted imaging is used to detect the characterization of HT (32). The presence of HT on brain image was determined by 2 neurologists independently, who were blinded to clinical outcome. When there was a disagreement between the 2 examiners, a decision was reached by consensus after joint review.

Laboratory Tests

12 h fasting blood samples were collected using ethylenediaminetetraacetic acid (EDTA) tubes on admission. Suspensions of plasma were centrifuged at 3000 g for 10 mins and immediately stored at -80℃ until analysis. The serum concentration of lipopolysaccharides (LPS) was measured with a Limulus amebocyte lysate assay (Houshiji Cod Inc., Xiamen, China). The amounts of LBP, sCD14, zonulin and Matrix metalloproteinase 9 (MMP9) in human plasma samples were measured using commercial kits according to the manufacturer's instructions (Cusabio Science Co, Ltd, Wuhan, China). The LBP and sCD14 levels in plasma of rats were determined using enzyme linked immunosorbent assay (ELISA) kits

according to the manufacturer's protocols (Elabscience, Wuhan, China). All the samples were run in duplicate.

Fecal DNA extraction and sequencing

Fresh stool samples were collected within 48 hours admission and stored at -80℃ until analysis. Total genome DNA from samples was extracted using CTBA method (33). DNA concentration and purity was monitored on 1% agarose gels. According to the concentration, DNA was diluted to 1ng/μL using sterile water. Variable regions V3-V4 of the bacterial 16S rRNA gene were amplified with degenerate polymerase chain reaction (PCR) primers. All PCR reactions were carried out with 15 μL of Phusion® High-Fidelity PCR Master Mix (New England Biolabs); 2 μM of forward and reverse primers, and about 10 ng template DNA. Thermal cycling consisted of initial denaturation at 98℃ for 1 min, followed by 30 cycles of denaturation at 98℃ for 10 s, annealing at 50℃ for 30 s, and elongation at 72℃ for 30 s. Finally 72℃ for 5 min. For the quantification and qualification of PCR products, mix same volume of 1X loading buffer (contained SYB green) with PCR products and operate electrophoresis on 2% agarose gel for detection. PCR products was mixed in equidensity ratios. Then, mixture PCR products was purified with Qiagen Gel Extraction Kit (Qiagen, Germany). Sequencing libraries were generated using TruSeq® DNA PCR-Free Sample Preparation Kit (Illumina, USA) following manufacturer's recommendations and index codes were added. The library quality was assessed on the Qubit@ 2.0 Fluorometer (Thermo Scientific) and Agilent Bioanalyzer 2100 system. At last, the library was sequenced on an Illumina MiSeq platform and 250 bp paired-end reads were generated.

Sequencing data analysis

Sequences were clustered into operational taxonomic units (OTUs) using the Upare software (34) (Uparse v7.0.1001, http://drive5.com/uparse/) . Sequences with ≥97% similarity were assigned to the same OTUs. Representative sequence for each OTU was screened for further annotation. For each representative sequence, the Silva Database (http://www.arb-silva.de/) was used based on Mothur algorithm to annotate taxonomic information (35). In order to study phylogenetic relationship of different OTUs, and the difference of the dominant species in different samples(groups), multiple sequence alignment were conducted using the MUSCLE software (Version 3.8.31 http://www.drive5.com/muscle/) (36). α diversity was assessed by two different parameters: the Shannon index (http://www.mothur.org/wiki/Shannon) and the Simpson index (http://www.mothur.org/wiki/Simpson). All these indices in our samples were calculated with QIIME (Version 1.7.0) and displayed with R software (Version 2.15.3). Beta diversity analysis was used to evaluate differences of samples in species complexity. Beta diversity on both weighted and unweighted unifrac were calculated by QIIME software (Version 1.9.1). Linear discriminant analysis (LDA) EffectSize Tools were used to compare the differences of microbial community compositions among groups (37). Finally, functional prediction was conducted by phylogenetic Investigation of Communities by Reconstruction of Unobserved States (PICRUSt) to identify enrichment of Kyoto Encyclopedia of Genes and Genomes (KEGG) pathways (38).

Animal care and experimental procedures

Male Sprague-Dawley (SD) rats were purchased from Hunan SJA Laboratory Animal Co. Ltd (Changsha, China) and kept under a 12 h light/12 h dark cycle in standard specific-pathogen-free (SPF) conditions. After acclimatization for 1 week, rats aged 7 weeks were randomly divided into experimental groups of six to eight mice, as follows: HT – infarct with hemorrhagic transformation; non-HT – infarct without hemorrhagic transformation; ABX – antibiotics-treated; non-ABX – control given by sterilized drinking water; F-HT – antibiotics-treated with fecal microbiota transplant from HT rats; F-non-HT – antibiotics-treated with fecal microbiota transplant from non-HT rats. All animal experimentation protocols were approved by the Institutional Animal Care and Use Committee of Central South University. All experiments were carried out according to animal experimentation animal welfare act guidelines.

The antibiotics treatment was performed and controlled as previously report (39, 40). To deplete gut flora, rats were given broad-spectrum antibiotics (vancomycin 0.5g/L, ampicillin 1g/L, metronidazole 1g/L, neomycin sulfate 1g/L; all from Meilun Biotechnology, Dalian, China) in drinking water for 4 weeks. The non-ABX group was received regular drinking water. ABX-containing water was replaced at every 3-4 d, together with the cage bedding. Rats in both groups were subjected to HT procedure after antibiotics treatment or not and then received regular or ABX-containing drinking water for the remainder of the experiment.

Fecal microbiota transplantation was performed as described elsewhere (41). After depletion of endogenous microbiota by antibiotics for 2 weeks, the rats were given by oral gavage once day with freshly extracted fecal microbiota from HT or non-HT rats. To obtain inoculants, 1 g of fresh feces from donor rats were pooled and suspended with 5 ml sterile PBS. The mixture was vortexed and centrifuged for 3 min at 1000 Í g, and the isolated supernatant was immediately given to recipient rats by oral gavage. Fresh feces were prepared within 15 minutes before oral gavage on the day of fecal transplantation. After administration fecal extract for 2 consecutive weeks, these recipients were experienced MCAO procedure. The rats were humanely euthanized on the 5^{th} day after MCAO procedure to collect blood sample, cecal contents and colon for next analysis. The LPS and LBP in the plasma was detected with ELISA as described above.

MCAO procedure and HT model

HT induction was performed as previously described (42). Rats received 50% dextrose (6ml/kg) intraperitoneally, 15 min before middle cerebral artery occlusion (MCAO), to induce acute hyperglycemia. Blood glucose was measured from the tail vein using a glucometer (Freestyle, Alameda, CA). During surgery and postoperative period, rectal temperature was maintained at 37.0℃ by using a feedback-controlled heating pad. Focal cerebral ischemia was performed as previously described (43). In brief, 90 min MCAO was performed under anesthesia followed by up to 5 days reperfusion. In order to expose the common carotid artery, external carotid artery (ECA) and internal carotid artery (ICA), a midline cervical incision was made. The ECA was separated and ligated. A rounded-tip 4-0 siliconized filament was

inserted into the internal carotid artery and advanced until the origin of the middle cerebral artery (MCA), approximately 18-22 mm from the insertion point, to produce a sudden drop of cerebral blood flow (CBF) to below 25% of baseline measured using a laser doppler monitor. Following MCAO, rats were placed in temperature-controlled recovery cages for 2 h to prevent post-surgery hypothermia. After 90 min, the occlusion suture was removed to allow reperfusion. Sham-operated rats underwent the same protocol of HT rats, without occlusion of the MCA. The survival of rats in each group was monitored daily.

Assessment of infarct volume and HT

Infarct volume was calculated 5 d after MCAO, as described previously (23). Brains were isolated, frozen on dry ice and serially sliced into 5 coronal sections (2-mm thick). The brain slices were stained with 1% 2,3,5-triphenyltetrazolium chloride (TTC, Sigma) for 15 min. The cerebral infarct area was calculated using Image J software 6.0 (Fig. 6D; red areas indicate no infarction, and white areas indicate infarction). In order to correct formula, the infarct area was calculated with the formula: the percentage of hemisphere lesion volume after edema correction = [total infarct volume - (ipsilateral hemisphere volume – contralateral hemisphere volume)]/contralateral hemisphere volume Í100%.

The stained brain sections are collected for hemoglobin content, quantified by spectrophotometric assay (43). After homogenization and centrifugation of brain tissue, the supernatant aliquots were collected. A 20-μL aliquot of supernatant was added with 80 μL of Drabkin reagent (Sigma) followed by optical density (OD) measurement at 540 nm. A blinded investigator scored macroscopic HT in brain slices using a four-point rubric (44), as follows: 0 – no hemorrhage; 1 – dispersed individual petechiae; 2 – confluent petechiae; 3 – small diffuse hemorrhage or hematoma; 4 – large diffuse hemorrhage or hematoma (Fig. 7F). The total score for each rat was reported.

Behavioral testing

Neurological function was assessed using Garcia score (45). The test was conducted 1, 3 and 5 d of reperfusion. The Garcia score is a composite of six parts: spontaneous activity, symmetry of movements (four limbs), symmetry of forelimbs (outstretching while held by tail); vibrissa touch, body proprioception, and the capacity of climb. Neurological function was graded on a scale of 0 to 18 points (normal score, 18; maximal deficit score, 3). The lower the score, the more severe the injury.

Sensorimotor deficits were assessed 2 and 4 d after MCAO surgery by the contact and removal adhesive tape test (46). Briefly, the rats were placed in a clear plexiglass box and allowed to explore the new environment for 2 or 3 min. A 10 mm diameter black color adhesive label was placed on the inside surface of each forelimb. Then we returned the rats to the plexiglass box and recorded the time for the rats to remove the first label and all other labels, respectively. Post-MCAO trials were conducted two times for 180 s each time to diminish stress effects related to handing. Results were expressed as mean of the two trials of either the contralateral contact or removal time. The two neurobehavioral tests were performed by investigators blinded to the experiments.

Western bolt analysis

Samples for western blot analysis were prepared as previously reported (47). The colon tissues were collected and lysed in SDS lysis buffer with the protease inhibitor phenylmethane sulfonyl fluoride (Beyotime Biotechnology, Beijng, China). BCA protein assay kit was used to measure the protein concentrations according to the manufacture's instructions. 5 × loading buffer (20% mercaptoethanol, 16% glycerol, 0.05% bromophenol blue, and 2% sodium dodecyl sulfate) was added to each sample before boiling for 5 min. The samples were stored at -80 °C until analysis. Equivalent amounts of protein (20 μg) were separated on sodium dodecyl sulfate polyacrylamide gel electrophoresis (SDS-PAGE). Then the membranes were incubated with primary antibodies at 4 °C overnight (anti-ZO1 tight junction antibody, 1:1000, Proteintech, Wuhan, China, 21773-1-AP; anti-TLR4 antibody, 1:1000, Proteintech, Wuhan, China, 19811-1-AP; anti-NF-κB p65 antibody, 1:1000, Proteintech, Wuhan, China, 10745-1-AP; anti-β-actin antibody, 1:10000, Cell Signaling Technology, MA, USA, BH10D10). The membranes were then washed in TBST and incubated with corresponding secondary antibody (goat anti-rabbit or mouse IgG, Jackson, 1:5000 dilution in blocking buffer) for 1 h at room temperature. The blots were quantified using the ChemiDoc MP System (Bio-Rad, Hercules, CA, USA). The band intensities of target protein were analyzed using Quantity One 4.4.0 software (Bio-Rad, Hercules, CA, USA). Outliers were excluded from the statistical analysis.

Statistical analysis

Data were analyzed using SPSS software 22.0 (IBM Corp., Armonk, NY, USA) and GraphPad Prism 9 (San Diego, CA, USA). A P value 0.05 was considered statistically significant. All of the data were tested for normality and variance homogeneity. Statistical significance between three groups was determined by a one-way analysis of variance (ANOVA) followed by post-hoc Tukey's multiple comparison test. Statistical comparisons between two groups were analyzed with Student's t-test. Nonparametric analyses were performed with Mann-Whitney U test (two groups) or the Kruskal-Wallis H test (three groups). The baseline characteristics of included patients were presented as number (%) and continuous variables with normal distributions were presented as the mean ± SD, while other variables that were not normally distributed were shown as the median (IQR). Patient characteristics were compared using the χ^2 test for trend for categorical data, one way ANOVA for normally distributed continuous data followed by the LSD test (equal variances assumed) or Tamhance's T2 test (equal variances not assumed), and the Kruskal–Wallis test for non-normally distributed continuous data. Spearman's correlation coefficient was used to analyzed the association between gut microbiota and plasma biomarkers.

Results

Participants' characteristics

A total of 48 participants were included in this study (Table 1). There are 15 patients with hemorrhagic transformation after stroke and 17 age- and sex-matched patients with AIS but without HT. The patients

in HT and non-HT group had a similar age and sex compared with controls. As expected, compared to non-HT patients, patients with HT presented with a more severe stroke (assessed using the National Institutes of Health Stroke Scale, NIHSS) (2 vs 6, p=0.005). The systolic blood pressure (SBP) at admission were significantly higher in patients with HT compared with HC (p=0.006). Recently, a study has shown that a high neutrophil- to-lymphocyte ratio predicts HT of large atherosclerotic infarction in patients with acute ischemic stroke (48). Consistently, in our results, the concentration of neutrophil and N to L ratio were also higher in HT group compared to HC group (p=0.027; p=0.005). N to L ratio was higher in HT group compared to non-HT group (p=0.012), suggesting that inflammatory response was associated with HT (p=0.027; p=0.005). Three participants were excluded due to low number of microbiome sequencing reads, resulting in a total of 43 participants included in the sequencing analyses below. Due to the small number of HT participants, we did not classify symptomatic and asymptomatic HT.

Gut microbiota profile of study participants

In total, 3659508 reads with read counts averaging 83316 reads per sample were denoised, merged, and survived chimera filtering. We quantified 2 commonly used metric for predicted gut microbiota studies, α- (ie, a within sample metrics) and β- (ie, a between sample metrics) diversity. As shown in Fig. 2A and 2B, compared to the controls, α and β diversity were decreased both in non-HT and HT group. But we did not observe differences in α and β diversity between non-HT and HT group. The overall microbial composition for HT and non-HT group were showed at the phylum, family, genus, and species levels (Fig. 2D, 2F, 2H, and Fig. S1B). The three largest phyla represented in each dataset of healthy controls, HT and non-HT groups were Firmicutes, Proteobacteria and Bacteroidetes while Pseudomonadaceae, Lachnospiraceae, and Enterobacteriaceae were the most abundant families (Fig. S1B and 2D). Ternary plot of phyla, family, and genus distribution across three groups showed Proteobacteria, Enterobacteriaceae, and Escherichia-Shigella (these three species belong to the same branch of the phylogenetic tree) were relatively more abundant in HT group than in the other two groups, respectively (Fig. S1A, 2C, and 2E). At the species level, Escherichia-coli was the predominate taxa in HT subjects (Fig. 2G). Species with significant differences ($p < 0.05$) among groups were marked with asterisk. Compared to the HC group, increased phylum Proteobacteria (p=0.015), decreased phyla Bacteroidota (p=0.021) and Actinobacteriota (p=0.024) were detected in the HT group (Fig. S1B). There are also some differences in phyla between HT and non-HT subjects. Chloroflexi (p=0.003), Myxococcota (p=0.002), Acidobacteriota (p=0.048), and unidentified_Bacteria (p=0.007) were increased, while the relative abundance of Campylobacterota (p□0.001) were decreased (Fig. S1B). At the family taxonomic level, we found increased relative abundance in Enterobacteriaceae (p=0.064) and decreased abundance in Muribaculaceae (p=0.023) and Lachnospiraceae (p=0.002) in the HT subjects compared to non-HT (Fig. 2D). Significantly increased relative abundance at genus and species level was Escherichia-Shigella (p=0.03) and Escherichia-Coli (p=0.025) respectively in HT group compared to non-HT group (Fig. 2F and 2H).

Some specific taxa were still more prevalent in non-HT group or HT group, shown by linear discriminant analysis scores higher than 3.5 in healthy controls, non-HT group or HT group (Fig. 3A and 3B). This cutoff was chosen specifically to identify taxa that were likely to have a biological significance instead of just significant *P* value. We identified that healthy subjects had higher levels of anti-inflammatory species including Ruminococcaceae, Acidobacteriota, Faecalibacterium, and Clostridiales, while non-HT subjects had higher levels of Streptococcus, Fusicatenibacter, and Pectobacterium, HT had higher levels of Lactobacillus_salivarius and Klebsiella (Fig. 3A and 3B). To find the groups which accounted for major differences in these three groups, we performed similarity percentage analysis (SIMPER) and obtained the sample dissimilarity contribution (Fig. 3C and 3D). Enterobacteriaceae at the family level and Escherichia-Shigella at the genus level were mostly accounted for major differences between the HT and non-HT groups. Network analysis also identified cooccurrence of bacterial taxa in different states. As shown in Fig. S2A, the network in HC subjects was dominant by a composed of beneficial Firmicutes. However, a highly complex network of interactions was found in HT group (Fig. S2C). The network in HT subjects was dominated by a chain of hub genera classified as Proteobacteria. Escherichia, the LPS-producing bacteria significantly increasing, cooccurred with different bacteria in HT network. As proposed in a previous study (49) that the positive and negative correlations represent metabolic complementarity and competition, respectively, it hinted that there was probably more competitive capacity for LPS-producing bacteria in HT subjects.

Microbial translocation and inflammatory response

Expect for the change of gut microbiota, the stroke patients challenged by HT also recapitulates some aspects of barrier dysfunctions associated with stroke. stroke patients with HT significantly increased MMP9 level in plasma compared to non-HT subjects (P=0.034, Fig. 4A). Meanwhile, the plasma concentration of zonulin was increased in HT group (P=0.029, Fig. 4B), suggesting the brain and gut barrier dysfunction. As a consequence of gut leakiness, microbial LPS released into tissues further stimulates TLR4 pathway in immune cells to promote subsequent systemic inflammation and neuroinflammation (50, 51). We quantified plasma levels of LPS as a maker of microbial translocation. The distribution of plasma LPS showed in Fig. 4C, was higher in HT subjects in comparison to non-HT subject ($p < 0.05$). To obtain further information concerning LPS in vivo, we also measured plasma sCD14 and LBP levels. LBP and sCD14 concentrations in both groups were exhibited in Fig. 4D and 4E. These values in HT group were different from the plasma sCD14 and LBP levels of non-HT group.

Next, we analyzed the associations between biomarker measurements and gut microbiota. As can be seen in Fig. 5A, plasma LPS (r=0.382, p=0.012) and zonulin (r=0.323, p=0.034) levels correlated positively with relative abundance of Escherichia-Shigella. In addition, we found a strong significant correlation between alpha diversity and LPS, as well as LBP (Fig. 5B). Higher levels of zonulin were negatively associated with Simple and Shannon index (Fig. 5B). So, it is reasonable to propose that LPS-related microbiota is associated with HT after stroke.

To determine whether predicted biological pathways with high sample prevalence rather than specific types of bacteria were associated with HT, we identified the predicted genes after passing QIIME-outputted amplicon sequence variant tables through the PICRUSt server (Fig. 5C). We identified 97 predicted microbiome gene pathways that were different as a result of the gut microbiota, 83 upregulated and 14 downregulated using PICRUSt. Particularly relevant were the upregulation of genes involved in the oxidative phosphorylation and biosynthesis of unsaturated fatty acids, all relevant to cardiovascular disease and stroke. PPAR signaling pathway, associated with both LPS and HT, was also upregulated in HT group. Moreover, we observed an increased trend in LPS-related functional pathways (LPS biosynthesis and LPS biosynthesis proteins) in HT participants compared to HC and non-HT subjects (Fig. 5D and 5E).

Microbiota-based regulation to HT

Consisted with our clinic findings, the relative abundance of Proteobacteria, Enterobacteriaceae, and Escherichia were also significantly increased in MCAO rats with hemorrhagic transformation in our previous research (28). To determine the role of gut microbiota and LPS-associated inflammation in HT process, we applied a HT mouse model (Fig. 6A). The HT group showed significantly larger infarct size ($p=0.005$, Fig. 6D) and severer neurological dysfunction than the non-HT group (Fig. 6F). Conformably, the hemoglobin content was also higher in HT group than in non-HT group ($p=0.023$, Fig. 6E). Additionally, motor and sensory impairment evaluated by adhesive removal test was carried out at two different time points (days 2 and 4; Fig. 6G and 6H). The HT group exhibited significantly increased time on the contact (Fig. 6G), longer time to remove the stickers (Fig. 6H). Concerning inflammatory factors, HT induced by hyperglycemia increased levels of the measured LPS ($p=0.04$), LBP and sCD14 ($p < 0.01$) in the plasma correspondingly to our clinical research (Fig. 6I to 6K). Compared to non-HT group, HT triggered an increase in LPS ($p=0.039$) and sCD14 ($p < 0.01$) concentration but no statistically significant changes in LBP concentration (Fig. 6I to 6K). The expression of ZO-1 protein remained significantly lower in HT group compared to the Sham group and non-HT group (Fig. 6L). Searching for the molecular mechanism, we quantified the levels of TLR4 and NF-κB, which has been reported to interacted with LPS and induce proinflammatory response (52). In general, TLR4 and NF-κB expression in HT group was higher than in non-HT group (Fig. 6L). Further, the mortality rate on the 5^{th} day was analyzed and exhibited a higher level in HT group compared to non-HT group ($p=0.026$, Fig. 6C).

In order to assess the role of gut microbiota in above-described intestinal microbiota in HT patients, we applied a rat model with depleted gut microbiota by treatment with a wide spectrum antibiotic cocktail. We submitted HT rats to antibiotics treatment (ABX group) and saline control (non-ABX group) (Fig. 7A). In accordance with our earlier report, ABX improved the neurologic impartment of HT rats assessed by Garcia score and adhesive tape test (Fig. 7H to 7J). The infarct volume and HT index were also slightly alleviated, yet, not statistically significantly (Fig. 7D and 7E). However, hemoglobin level in ABX was reduced ($p=0.018$, Fig. 7G). Accordingly, the augment in LPS ($p=0.038$) and LBP ($p=0.049$) level in ABX compared to non-ABX was lessened by doing antibiotics (Fig. 7K and 7L). The concentration of sCD14 was not affect by microbiota depletion (Fig. 7M). HT-elicited differences in TLR4 and NF-κB protein

expression were offset by bacteria depletion (Fig. 7N). The HT animals with depleted intestinal microbiota show significant differences in ZO-1 protein expression compared to non-ABX rats (Fig. 7N). In ABX animals, the mortality rate (27.3 % vs 64.3%, Fig. 7C) was reduced compared to non-ABX rats, but was not statistically significant.

In order to confirm the role of microbiota, we performed fecal transplants from HG and NG rats to another group of rats with depleted bacteria and made MCAO procedure (F-HT, F-non-HT) (Fig. 8A). Compared to F-non-HT group, microbiota transplant from HG rats experienced an increase in infarct volume ($p=0.034$), HT index ($p < 0.01$), and hemoglobin level ($p=0.023$) (Fig. 8D to 8F). The rats in F-HT group showed remarkable worsening in the adhesive removal test compared to the rats in F-non-HT group (Fig. 8G to 8I). Microbiota transplant from HG triggered a higher level of LPS ($p < 0.01$), LBP ($p=0.022$) and sCD14 ($p < 0.01$) in plasma (Fig. 8J to 8L). In the colon tissue, the expression of ZO-1 protein was decreased in F-HT compared to F-non-HT rats (Fig. 8M), demonstrating that the destructive intestinal barrier in F-HT group. The expression of TLR4 and NF-κB protien in colon tissue was higher in F-HT rats compared to F-non-HT rats (Fig. 8M). Not surprisingly, the mortality rate was higher in FMT-HG group, yet, not statistically significant ($p=0.4$, Fig. 8C).

Discussion

Here, we combined gut microbiota sequencing and LPS, LBP, as well as sCD14 quantification with HT monitoring from a retrospective cohort. Our study uncovered that gut microbiota of HT and non-HT group is different from healthy subjects in terms of the diversity and composition. There are some special bacteria in HT group, such as the increased Escherichia–Shigella and Coli. Moreover, we found that HT participants had higher levels of LPS, LBP and sCD14 in plasma. The expression of TLR4 and NF-κB protien in colon tissue are also different. In experimental research, we administrated the rats with antibiotics and microbiol transplant and verified the role of gut microbiota in HT process. Taken together, our study uncovered LPS-induced inflammatory pathway mediated by the gut microbiota of HT patients that may drive an increased risk in HT and could form new therapeutic approaches for hemorrhagic transformation (summarized in Fig. 9).

This bidirectional communication, termed the microbiota-gut-brain (MGB) axis, provides novel avenues for both the prevention and treatment of stroke (53-57). In accordance with these prior studies, we observe a change in microbial α and β diversity between HC and non-HT or HT groups. Albeit we did not identify diversity changes between non-HT and HT groups, we still identified some differentially prevalent taxa. Particularly relevant are the higher levels of Escherichia–Shigella and Coli observed in HT subjects. Enterobacteriaceae is known as LPS-producers and have been previously positively associated with stroke in other cohorts (7, 26). In our sequencing results, we found that the relative abundance of Escherichia was significantly higher in HT subjects than in non-HT subjects. In order to confirm the role of microbiota, we performed fecal transplants and antibiotics treatment. Crucially, treatment with antibiotics partly improves the tested parameters including infarct volume and behavior test affected by HT presentation. The transplant of the microbiota of HT donors aggravates infarct severity of MCAO rats to a

certain extend. It has previously been reported that microbiota plays a vital role in stroke (8, 58) and its complications, including stroke depression (59), cognitive impairment (60, 61), infection (62), etc. Therefore, the here presented data adds a fitting piece to a picture of microbiota-based response to stroke outcomes.

Gut microbial metabolites are key for gut microbiota-host communication. One of the gene pathways we identified was an upregulation of LPS biosynthesis and LPS biosynthesis proteins but not statistically significant in HT subjects. Indeed, we found higher levels of LPS and LBP in HT subjects. LBP is produced by hepatic and gastrointestinal epithelial cells in response to LPS stimulation (63). LBP and sCD14 belongs to acute phase proteins and are considered as makers of LPS bioactivity (64). In an inflammatory stimulus, LBP binds to LPS and delivers them to CD14, which is a pattern-recognition receptor associated with E.coli and participates in the LPS signaling (9). In our study, compared to the non-HT and healthy controls, HT subjects had higher LPS and LBP levels, demonstrating that LPS-induced inflammatory response is associated with HT process. Furthermore, we verified the role of gut microbiota and LPS in HT process by antibiotic treatment and microbial transplantation. Antibiotic cocktail suppressed LPS and LBP generation significantly, along with TLR4 and NF-κB protein in colon, the well-known inflammatory signaling. Then, the “conventionalized” rats (with the gut flora rescued) showed increased plasma LPS and LBP level. Our results link endotoxin-related inflammation to the risk of HT and gut dysbiosis after stroke, but the casual evidence among these factors should be further explored.

Upregulation of LPS-TLR4 signaling results in immune dysfunction which drives a shift to a pro-inflammatory phenotype including recruitment of neutrophils and other immune cells. A greater peripheral neutrophil-to-lymphocyte ratio was found among HT subjects proving inflammation exists in HT patients and at least involves an increase in neutrophils (65). A retrospective study of 270 HT patients also investigates high neutrophile-to-platelet ratio is associated with HT (66). In our previous study, we have found that the level of proinflammatory cytokines including TNF-α, IL-1β, IL-17 were higher in HT rats than non-HT rats, suggesting a pro-inflammatory status under HT conditions (28). In the precent study, we also propose a HT model in which upon increased concentration of LPS and LBP after MCAO procedure, microbiota acts to mediate LPS-induced inflammatory response and therefore raises the levels of proinflammatory factors. The increased appearance of LPS-induced inflammation may be executed by TLR4, leading to the activation of NF-κB signaling. Thus, the upregulation of LPS-TLR4 pathway may be (partially) responsible for the proinflammatory phenotype (increase in neutrophils and N to L ratio) observed in HT subjects. In the future, coupling the immune phenotype of subjects with LPS-sensing TLR4 expression is needed to further understand how LPS-signaling affects the various immune cells.

The integrity of barrier about brain and gut mediates neuroinflammation and systemic inflammation after stroke (67). The blood-brain barrier (BBB) is considered as the gatekeeper of the CNS, whose main role is to maintain the fragile homeostasis of the brain. The cascade related to reperfusion injury and oxidative stress, leukocyte infiltration and dysregulated extracellular proteolysis contributes to HT by undermining the integrity of BBB (68). High MMP-9 levels has been evidenced as independently predicted factor for HT

in stroke patients (69). Otherwise, it is increasingly evident that stroke alters gut motility and increases gut permeability (22), which allows LPS to enter the bloodstream and activates vascular inflammation (58). Recently, Carloni et al. has identified that bacteria-derived LPS contributes to deregulated gut-brain vascular barrier and inflammatory bowl disease-related mental symptoms (27). Of note, in our present findings, both zonulin and MMP9 level in stroke patients with HT were decreased, suggesting a compromised intestinal and brain barrier. We found that ZO-1 expression is decreased in HT rats, which supports the dysfunction of gut barrier. Interestingly, microbiota transplant triggered greater changes in ZO-1 expression of colon tissue. The antibiotics treatment of HG rats adjusted the levels of ZO-1 protein. Still, more research is required to verify how HT-induced changes in special gut microbiota and LPS affect the integrity of BBB and intestinal barrier.

There are some limitations to our study. This is a single center study with recruiting relatively small sample size. However, it can be emphasized that our results are consistent with previous studies as to risk factors for HT. As a results of the detailed characterization of this cohort including excluding diabetes, which belongs to the major comorbidity of stroke, especially LAA subtypes, our results are robust and valid to show the relationship between gut microbiota and HT. Albeit modest, our study took advantage of the cohort and animal model of stroke, which allowed us to determine microbial associations in HT process.

Conclusions

In conclusion, we identified that while microbial diversity did not change in HT subjects compared to non-HT subjects, there was a significant shift in composition of gut microbiota involved in HT. The concentration of LPS was increased, coupled with upregulated TLR4 signaling. This suggests that targeting LPS-TLR4 pathway and special bacteria identified here may represent new avenues in the search for mechanisms that control HT in stroke patients.

Abbreviations

BBB: Blood-brain barrier; FBG: Fasting blood glucose; HC: Healthy controls; HT: Hemorrhagic transformation; HDL: High-density lipoprotein; LBP: LPS-binding protein; LDA: Linear discriminant analysis; LDL: Low-density lipoprotein; LPS: lipopolysaccharide; MCAO: middle cerebral artery occlusion; MGB: microbiota-gut-brain; MMP9: Matrix metalloproteinase 9; N/L: Neutrophil- to-lymphocyte ratio; OTUs: operational taxonomic units; SBP: Systolic blood pressure; sCD14: solube CD14; TC: Cholesterol; TG: Triglycerides; TLR4: Toll-like receptor 4; ZO-1: Zonulin.

Declarations

Supplemental material

Supplemental material is available online only. Additional supporting information may be found online in the supporting information section.

Acknowledgments

We thank all patients for their participation in this study. We declare no conflicts of interest.

Disclosure

None.

Authors' contributions

QH and JX designed the experiments and conducted the study. QH wrote the manuscript. JX revised the manuscript. QH and DL contributed to the animal experiment. MPW and XJF contributed to literature search, data collection, analysis and interpretation. FY and ZYL provided technical support. QH and YHL contributed to the sample collection in patients. YFL, RXT, and TTZ performed sample collection and statistical analysis. All authors read and approved the final manuscript.

Funding

This study was supported by the Project Program of National Clinical Research Center for Geriatric Disorders (Xiangya Hospital, Grant No. 2020LNJJ16), the National Natural Science Foundation of China (Grant No. 81671166), the Fundamental Research Funds for the Central Universities of Central South University (Grant No. 2019ZZTS902), and the Provincial Key Plan for Research and Development of Hunan (Grant No. 2020SK2067).

Data availability statement

All data are in the manuscript and the associated supporting information file. The datasets generation for this study can be found in the NCBI (https://www.ncbi.nlm.nih.gov/; BioProject: PRJNA783129).

Ethics approval and consent to participate

All animal experiments were approved by the Institutional Animal Care and Use Committee of Central South University. The clinical study was approved by the Ethics Committee of Xiangya Hospital of Central South University.

Consent for publication

Not applicable.

Competing interests

All authors declare no competing interests.

ORCID

Jian Xia https://orcid.org/0000-0001-9154-131X

References

1. Wang XY, Lo EH. Triggers and mediators of hemorrhagic transformation in cerebral ischemia. Molecular Neurobiology. 2003;28(3):229-44.
2. Thiebaut AM, Gauberti M, Ali C, Martinez De Lizarrondo S, Vivien D, Yepes M, et al. The role of plasminogen activators in stroke treatment: fibrinolysis and beyond. The Lancet Neurology. 2018;17(12):1121-32.
3. El-Zammar ZMK, Levine SR. IS ASYMPTOMATIC HEMORRHAGIC TRANSFORMATION REALLY INNOCUOUS? Neurology. 2012;78(21):1704-.
4. Jickling GC, Ander BP, Stamova B, Zhan X, Liu D, Rothstein L, et al. RNA in blood is altered prior to hemorrhagic transformation in ischemic stroke. Ann Neurol. 2013;74(2):232-40.
5. Brown GC. The endotoxin hypothesis of neurodegeneration. J Neuroinflammation. 2019;16(1):180.
6. Macrez R, Ali C, Toutirais O, Le Mauff B, Defer G, Dirnagl U, et al. Stroke and the immune system: from pathophysiology to new therapeutic strategies. The Lancet Neurology. 2011;10(5):471-80.
7. Kurita N, Yamashiro K, Kuroki T, Tanaka R, Urabe T, Ueno Y, et al. Metabolic endotoxemia promotes neuroinflammation after focal cerebral ischemia. Journal of Cerebral Blood Flow & Metabolism. 2020;40(12):2505-20.
8. Guo Q, Jiang X, Ni C, Li L, Chen L, Wang Y, et al. Gut Microbiota-Related Effects of Tanhuo Decoction in Acute Ischemic Stroke. Oxid Med Cell Longev. 2021;2021:5596924.
9. Laugerette F, Alligier M, Bastard JP, Drai J, Chanseaume E, Lambert-Porcheron S, et al. Overfeeding increases postprandial endotoxemia in men: Inflammatory outcome may depend on LPS transporters LBP and sCD14. Mol Nutr Food Res. 2014;58(7):1513-8.
10. Jack RS, Grunwald U, Stelter F, Workalemahu G, Schutt C. BOTH MEMBRANE-BOUND AND SOLUBLE FORMS OF CD14 BIND TO GRAM-NEGATIVE BACTERIA. European Journal of Immunology. 1995;25(5):1436-41.
11. Beschorner R, Nguyen TD, Gozalan F, Pedal I, Mattern R, Schluesener HJ, et al. CD14 expression by activated parenchymal microglia/macrophages and infiltrating monocytes following human traumatic brain injury. Acta Neuropathologica. 2002;103(6):541-9.
12. Cauwels A, Frei K, Sansano S, Fearns C, Ulevitch R, Zimmerli W, et al. The origin and function of soluble CD14 in experimental bacterial meningitis. Journal of Immunology. 1999;162(8):4762-72.
13. Haziot A, Ferrero E, Kontgen F, Hijiya N, Yamamoto S, Silver J, et al. Resistance to endotoxin shock and reduced dissemination of gram-negative bacteria in CD14-deficient mice. Immunity. 1996;4(4):407-14.

14. Klimiec E, Pera J, Chrzanowska-Wasko J, Golenia A, Slowik A, Dziedzic T. Plasma endotoxin activity rises during ischemic stroke and is associated with worse short-term outcome. J Neuroimmunol. 2016;297:76-80.
15. Aune SK, Cwikiel J, Flaa A, Arnesen H, Solheim S, Awoyemi A, et al. Gut Leakage Markers in Response to Strenuous Exercise in Patients with Suspected Coronary Artery Disease. Cells. 2021;10(9).
16. Sun L, Yu Z, Ye X, Zou S, Li H, Yu D, et al. A marker of endotoxemia is associated with obesity and related metabolic disorders in apparently healthy Chinese. Diabetes Care. 2010;33(9):1925-32.
17. Safadi JM, Quinton AMG, Lennox BR, Burnet PWJ, Minichino A. Gut dysbiosis in severe mental illness and chronic fatigue: a novel trans-diagnostic construct? A systematic review and meta-analysis. Mol Psychiatry. 2021.
18. Brea D, Poon C, Benakis C, Lubitz G, Murphy M, Iadecola C, et al. Stroke affects intestinal immune cell trafficking to the central nervous system. Brain Behav Immun. 2021;96:295-302.
19. Collins SM, Surette M, Bercik P. The interplay between the intestinal microbiota and the brain. Nat Rev Microbiol. 2012;10(11):735-42.
20. Zeng X, Gao X, Peng Y, Wu Q, Zhu J, Tan C, et al. Higher Risk of Stroke Is Correlated With Increased Opportunistic Pathogen Load and Reduced Levels of Butyrate-Producing Bacteria in the Gut. Front Cell Infect Microbiol. 2019;9:4.
21. Zhu W, Romano KA, Li L, Buffa JA, Sangwan N, Prakash P, et al. Gut microbes impact stroke severity via the trimethylamine N-oxide pathway. Cell Host Microbe. 2021;29(7):1199-208 e5.
22. Lee J, d'Aigle J, Atadja L, Quaicoe V, Honarpisheh P, Ganesh BP, et al. Gut Microbiota-Derived Short-Chain Fatty Acids Promote Poststroke Recovery in Aged Mice. Circ Res. 2020;127(4):453-65.
23. Zhang P, Zhang X, Huang Y, Chen J, Shang W, Shi G, et al. Atorvastatin alleviates microglia-mediated neuroinflammation via modulating the microbial composition and the intestinal barrier function in ischemic stroke mice. Free Radic Biol Med. 2021;162:104-17.
24. Haak BW, Westendorp WF, van Engelen TSR, Brands X, Brouwer MC, Vermeij JD, et al. Disruptions of Anaerobic Gut Bacteria Are Associated with Stroke and Post-stroke Infection: a Prospective Case-Control Study. Transl Stroke Res. 2021;12(4):581-92.
25. Yin J, Liao SX, He Y, Wang S, Xia GH, Liu FT, et al. Dysbiosis of Gut Microbiota With Reduced Trimethylamine-N-Oxide Level in Patients With Large-Artery Atherosclerotic Stroke or Transient Ischemic Attack. J Am Heart Assoc. 2015;4(11).
26. Xu K, Gao X, Xia G, Chen M, Zeng N, Wang S, et al. Rapid gut dysbiosis induced by stroke exacerbates brain infarction in turn. Gut. 2021.
27. Carloni S, Bertocchi A, Mancinelli S, Bellini M, Erreni M, Borreca A, et al. Identification of a choroid plexus vascular barrier closing during intestinal inflammation. Science (New York, NY). 2021;374(6566):439-48.
28. Huang Q, Di L, Yu F, Feng X, Liu Z, Wei M, et al. Alterations in the gut microbiome with hemorrhagic transformation in experimental stroke. CNS Neurosci Ther. 2021.

29. Adams HP, Bendixen BH, Kappelle LJ, Biller J, Love BB, Gordon DL, et al. CLASSIFICATION OF SUBTYPE OF ACUTE ISCHEMIC STROKE - DEFINITIONS FOR USE IN A MULTICENTER CLINICAL-TRIAL. Stroke. 1993;24(1):35-41.
30. Brott T, Adams HP, Olinger CP, Marler JR, Barsan WG, Biller J, et al. MEASUREMENTS OF ACUTE CEREBRAL INFARCTION - A CLINICAL EXAMINATION SCALE. Stroke. 1989;20(7):864-70.
31. Motto C, Ciccone A, Aritzu E, Boccardi E, De Grandi C, Piana A, et al. Hemorrhage after an acute ischemic stroke. Stroke. 1999;30(4):761-4.
32. Renou P, Sibon I, Tourdias T, Rouanet F, Rosso C, Galanaud D, et al. Reliability of the ECASS radiological classification of postthrombolysis brain haemorrhage: a comparison of CT and three MRI sequences. Cerebrovasc Dis. 2010;29(6):597-604.
33. Caporaso JG, Kuczynski J, Stombaugh J, Bittinger K, Bushman FD, Costello EK, et al. QIIME allows analysis of high-throughput community sequencing data. Nature Methods. 2010;7(5):335-6.
34. Edgar RC. UPARSE: highly accurate OTU sequences from microbial amplicon reads. Nature Methods. 2013;10(10):996-+.
35. Quast C, Pruesse E, Yilmaz P, Gerken J, Schweer T, Yarza P, et al. The SILVA ribosomal RNA gene database project: improved data processing and web-based tools. Nucleic acids research. 2013;41(Database issue):D590-6.
36. Edgar RC. MUSCLE: multiple sequence alignment with high accuracy and high throughput. Nucleic Acids Research. 2004;32(5):1792-7.
37. Segata N, Izard J, Waldron L, Gevers D, Miropolsky L, Garrett WS, et al. Metagenomic biomarker discovery and explanation. Genome Biol. 2011;12(6):R60.
38. Langille MG, Zaneveld J, Caporaso JG, McDonald D, Knights D, Reyes JA, et al. Predictive functional profiling of microbial communities using 16S rRNA marker gene sequences. Nat Biotechnol. 2013;31(9):814-21.
39. Brown RL, Sequeira RP, Clarke TB. The microbiota protects against respiratory infection via GM-CSF signaling. Nat Commun. 2017;8(1):1512.
40. Huang HI, Jewell ML, Youssef N, Huang MN, Hauser ER, Fee BE, et al. Th17 Immunity in the Colon Is Controlled by Two Novel Subsets of Colon-Specific Mononuclear Phagocytes. Front Immunol. 2021;12:661290.
41. Sorini C, Cosorich I, Lo Conte M, De Giorgi L, Facciotti F, Luciano R, et al. Loss of gut barrier integrity triggers activation of islet-reactive T cells and autoimmune diabetes. Proc Natl Acad Sci U S A. 2019;116(30):15140-9.
42. Hafez S, Hoda MN, Guo X, Johnson MH, Fagan SC, Ergul A. Comparative Analysis of Different Methods of Ischemia/Reperfusion in Hyperglycemic Stroke Outcomes: Interaction with tPA. Transl Stroke Res. 2015;6(3):171-80.
43. Guo ZN, Xu L, Hu Q, Matei N, Yang P, Tong LS, et al. Hyperbaric Oxygen Preconditioning Attenuates Hemorrhagic Transformation Through Reactive Oxygen Species/Thioredoxin-Interacting

Protein/Nod-Like Receptor Protein 3 Pathway in Hyperglycemic Middle Cerebral Artery Occlusion Rats. Crit Care Med. 2016;44(6):e403-11.

44. Kelly-Cobbs AI, Prakash R, Li W, Pillai B, Hafez S, Coucha M, et al. Targets of vascular protection in acute ischemic stroke differ in type 2 diabetes. Am J Physiol Heart Circ Physiol. 2013;304(6):H806-15.
45. Garcia JH, Wagner S, Liu KF, Hu XJ. NEUROLOGICAL DEFICIT AND EXTENT OF NEURONAL NECROSIS ATTRIBUTABLE TO MIDDLE CEREBRAL-ARTERY OCCLUSION IN RATS - STATISTICAL VALIDATION. Stroke. 1995;26(4):627-34.
46. Luo M, Tang X, Zhu J, Qiu Z, Jiang Y. Establishment of Acute Pontine Infarction in Rats by Electrical Stimulation. J Vis Exp. 2020(162).
47. Wang Z, Chen W-H, Li S-X, He Z-M, Zhu W-L, Ji Y-B, et al. Gut microbiota modulates the inflammatory response and cognitive impairment induced by sleep deprivation. Molecular Psychiatry. 2021.
48. Zhang W-B, Zeng Y-Y, Wang F, Cheng L, Tang W-J, Wang X-Q. A high neutrophil-to-lymphocyte ratio predicts hemorrhagic transformation of large atherosclerotic infarction in patients with acute ischemic stroke. Aging-Us. 2020;12(3):2428-39.
49. Levy R, Borenstein E. Metabolic modeling of species interaction in the human microbiome elucidates community-level assembly rules. Proc Natl Acad Sci U S A. 2013;110(31):12804-9.
50. Al-Asmakh M, Hedin L. Microbiota and the control of blood-tissue barriers. Tissue Barriers. 2015;3(3):e1039691.
51. Houser MC, Tansey MG. The gut-brain axis: is intestinal inflammation a silent driver of Parkinson's disease pathogenesis? NPJ Parkinsons Dis. 2017;3:3.
52. Liu T, Zhang L, Joo D, Sun SC. NF-kappaB signaling in inflammation. Signal Transduct Target Ther. 2017;2.
53. Benakis C, Brea D, Caballero S, Faraco G, Moore J, Murphy M, et al. Commensal microbiota affects ischemic stroke outcome by regulating intestinal gammadelta T cells. Nat Med. 2016;22(5):516-23.
54. Jeon J, Lourenco J, Kaiser EE, Waters ES, Scheulin KM, Fang X, et al. Dynamic Changes in the Gut Microbiome at the Acute Stage of Ischemic Stroke in a Pig Model. Front Neurosci. 2020;14:587986.
55. Singh V, Roth S, Llovera G, Sadler R, Garzetti D, Stecher B, et al. Microbiota Dysbiosis Controls the Neuroinflammatory Response after Stroke. J Neurosci. 2016;36(28):7428-40.
56. Stanley D, Moore RJ, Wong CHY. An insight into intestinal mucosal microbiota disruption after stroke. Sci Rep. 2018;8(1):568.
57. Wang H, Song W, Wu Q, Gao X, Li J, Tan C, et al. Fecal Transplantation from db/db Mice Treated with Sodium Butyrate Attenuates Ischemic Stroke Injury. Microbiol Spectr. 2021;9(2):e0004221.
58. Brown JM, Hazen SL. The gut microbial endocrine organ: bacterially derived signals driving cardiometabolic diseases. Annu Rev Med. 2015;66:343-59.
59. Jiang W, Gong L, Liu F, Ren Y, Mu J. Alteration of Gut Microbiome and Correlated Lipid Metabolism in Post-Stroke Depression. Front Cell Infect Microbiol. 2021;11:663967.

60. Ling Y, Gong T, Zhang J, Gu Q, Gao X, Weng X, et al. Gut Microbiome Signatures Are Biomarkers for Cognitive Impairment in Patients With Ischemic Stroke. Front Aging Neurosci. 2020;12:511562.
61. Liu Y, Kong C, Gong L, Zhang X, Zhu Y, Wang H, et al. The Association of Post-Stroke Cognitive Impairment and Gut Microbiota and its Corresponding Metabolites. J Alzheimers Dis. 2020;73(4):1455-66.
62. Stanley D, Mason LJ, Mackin KE, Srikhanta YN, Lyras D, Prakash MD, et al. Translocation and dissemination of commensal bacteria in post-stroke infection. Nat Med. 2016;22(11):1277-84.
63. Park BS, Lee JO. Recognition of lipopolysaccharide pattern by TLR4 complexes. Exp Mol Med. 2013;45:e66.
64. Schumann RR, Zweigner J. A novel acute-phase marker: Lipopolysaccharide binding protein (LBP). Clinical Chemistry and Laboratory Medicine. 1999;37(3):271-4.
65. Switonska M, Piekus-Slomka N, Slomka A, Sokal P, Zekanowska E, Lattanzi S. Neutrophil-to-Lymphocyte Ratio and Symptomatic Hemorrhagic Transformation in Ischemic Stroke Patients Undergoing Revascularization. Brain Sci. 2020;10(11).
66. He W, Ruan Y, Yuan C, Cheng Q, Cheng H, Zeng Y, et al. High Neutrophil-to-Platelet Ratio Is Associated With Hemorrhagic Transformation in Patients With Acute Ischemic Stroke. Front Neurol. 2019;10:1310.
67. Zhu S, Jiang Y, Xu K, Cui M, Ye W, Zhao G, et al. The progress of gut microbiome research related to brain disorders. J Neuroinflammation. 2020;17(1):25.
68. Khatri R, McKinney AM, Swenson B, Janardhan V. Blood-brain barrier, reperfusion injury, and hemorrhagic transformation in acute ischemic stroke. Neurology. 2012;79(13):S52-S7.
69. Castellanos M, Leira R, Serena J, Pumar JM, Lizasoain I, Castillo J, et al. Plasma metalloproteinase-9 concentration predicts hemorrhagic transformation in acute ischemic stroke. Stroke. 2003;34(1):40-5.

Table

Table 01

Characteristics	HC n=16	non-HT n=17	HT n=15	P-value
Age, year (mean±SD)	57.63±9.66	60.47±7.69	64.6±12.92	0.173
Sex (% female)	7 (43.8)	5 (29.4)	6 (40)	0.677
History of hypertension (%)	1 (6.3)	13 (76.5) ‡	10 (66.7) ‡	0.001
History of smoking (%)	4 (25.0)	9 (52.9)	4 (26.7)	0.170
History of drinking (%)	2 (12.5)	7 (41.2)	5 (33.3)	0.177
HDL (mmol/L)	1.11±0.25	1.11±0.25	1.18±0.38	0.729
LDL (mmol/L)	3.18±0.63	2.80±0.60	3.34±0.96	0.116
TC (mmol/L)	4.88±0.86	4.40±0.79	4.71±1.41	0.406
TG (mmol/L)	2.01±1.45	1.51±0.61	1.46±0.77	0.242
FBG (mmol/L)	6.29±1.31	7.29±1.71	6.87±1.58	0.187
Baseline NIHSS score (IQR)	-	2 (5)	6 (10) §	0.005
Systolic blood pressure (mmHg)	130.69±17.4	142.12±16.23	149.13±19.6 ‡	0.019
Diastolic blood pressure (mmHg)	84.31±9.99	86.12±11.1	83.93±14.21	0.853
Neutrophil (× 10^9)	3.25±1.01	4.18±1.35	5.33±2.59‡	0.007
Lymphocyte (× 10^9)	1.50±0.37	1.78±0.44	1.52±0.53	0.147
N/L	2.32±0.96	2.51±1.04	3.90±2.23‡§	0.01

Demographics and Clinical Characteristics of Participants. Continuous data are presented as mean ± standard deviation or median (interquartile range), categorical variables are presented as %. FBG, fasting blood glucose; TG, triglycerides; TC, cholesterol; HDL, high-density lipoprotein; LDL, low-density lipoprotein; N/L, neutrophil- to-lymphocyte ratio; HC, healthy controls; HT, hemorrhagic transformation group; non-HT, non-hemorrhagic transformation group. The p-values of gender and dietary habits were determined by Pearson's chi-square test. ‡ p0.05 when compared with HC group, § p0.05 when compared with non-HT group.

Figures

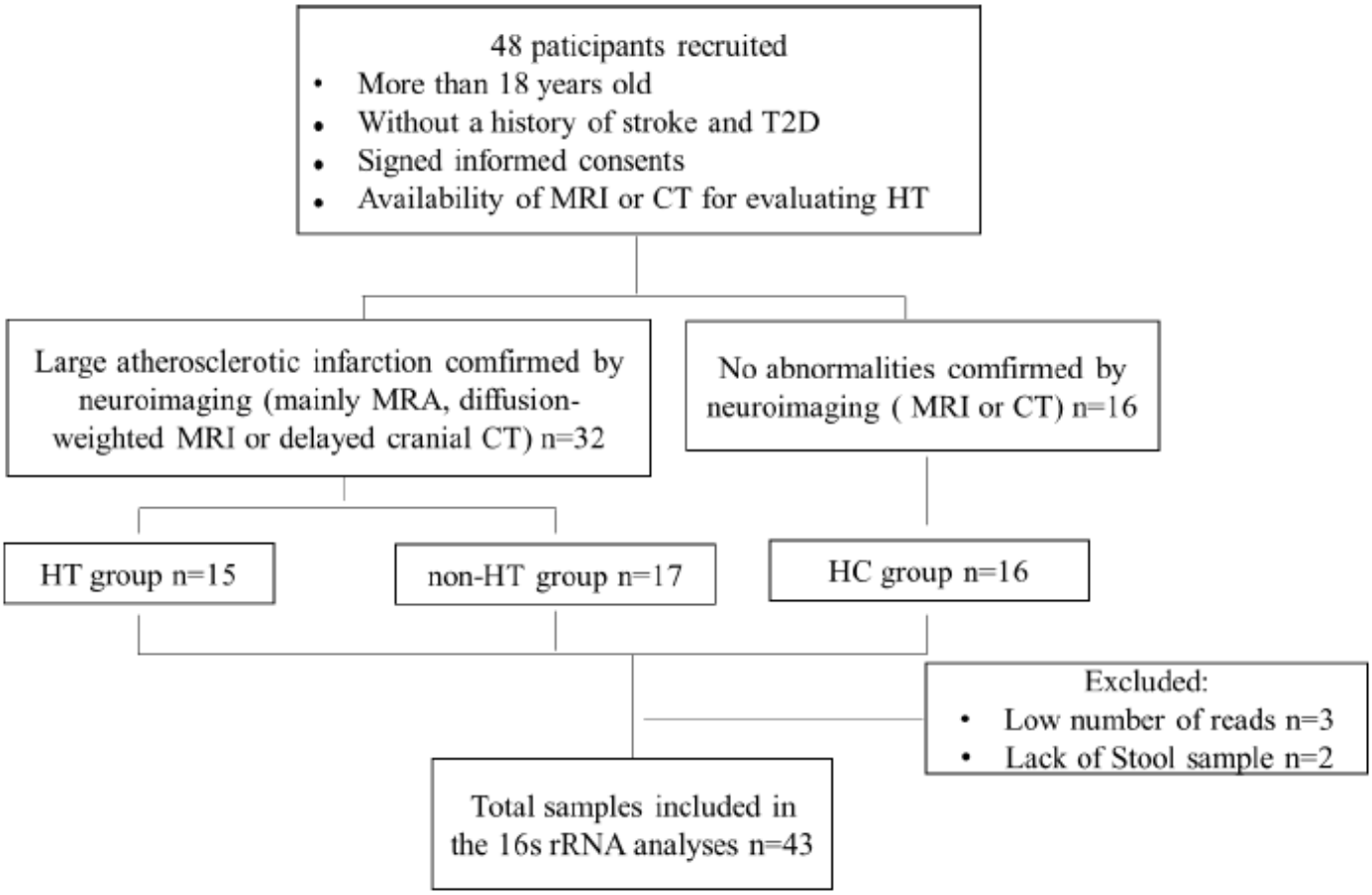

Figure 1

The flowchart in this study. Legend: HC: healthy controls; HT, stroke patients with hemorrhagic transformation; non-HT: stroke patients without hemorrhagic transformation.

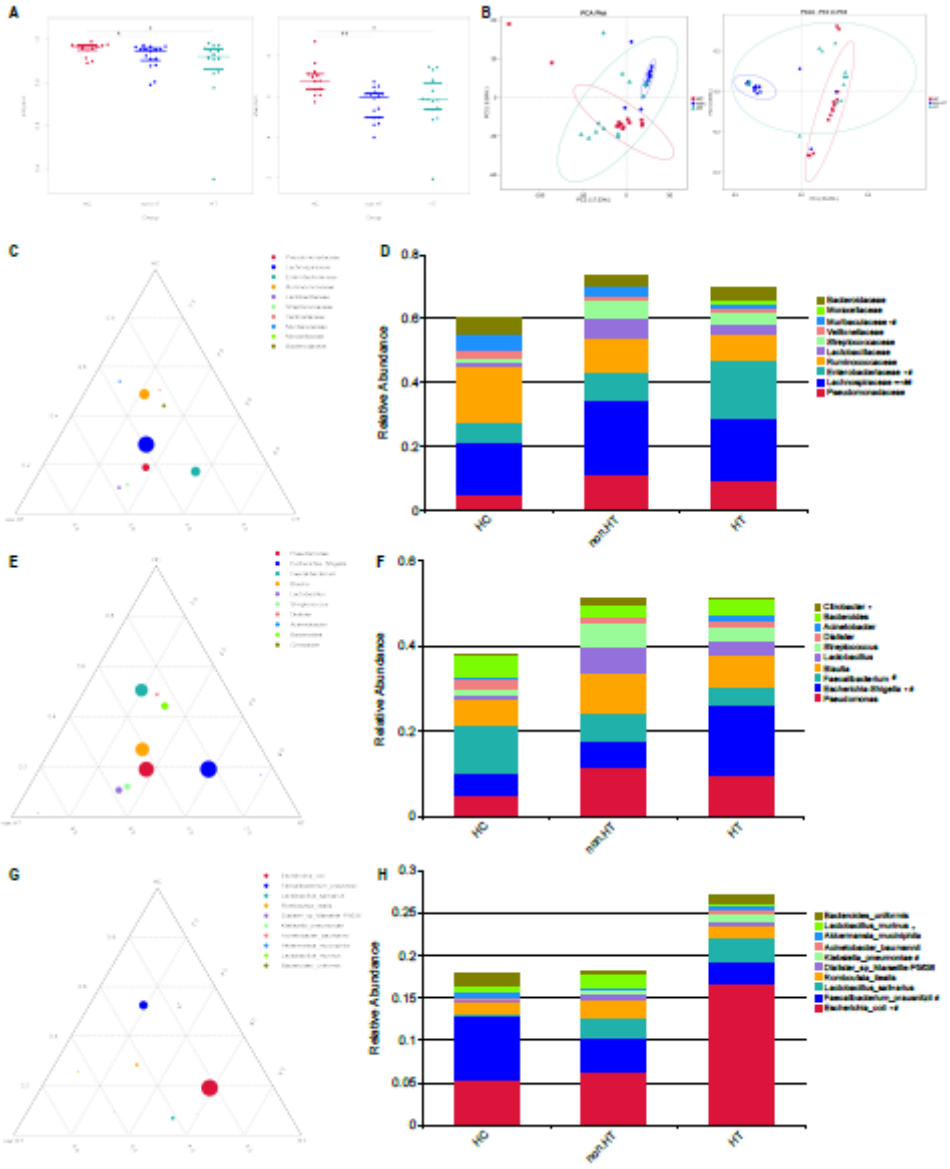

Figure 2

Gut dysbiosis of HT subjects. (A). Analysis of alpha diversity of gut microbiota by Shannon (left) and Simpson (right) analysis. (B). (left) β diversity principal coordinate analysis plot based on unweighted (i.e., microbial diversity based on presence/absence) UniFrac analyses showing difference in the gut microbiome between HC and stroke patients, but showing no difference between HT and non-HT subjects (Anosim analysis: $r > 0$; $p < 0.05$). (right) Principal component analysis of beta diversity in different groups. (C, E, and G). Ternary plot of OTU distribution reflecting predominant taxa across three groups at the family level (C), genus level (E), and species level (G). Each circle represents one OTU, and the size, color and position of the circle represent its relative abundance, bacterial phylum and affiliation of the OTU with the different regions, respectively. (D, F, and H) Average relative abundances of bacterial phyla distributed in HC, HT, and non-HT group. Top 10 relative abundance at family level (D), genus level (F), and species level (H) (average relative abundance above 1%) with significantly differential distribution (as

detected by MetaStat analysis) are marked with asterisk. #P < 0.05, ##P < 0.01, ###P < 0.001 versus HC group; *P < 0.05, **P < 0.01, ***P < 0.001 versus non-HT group.

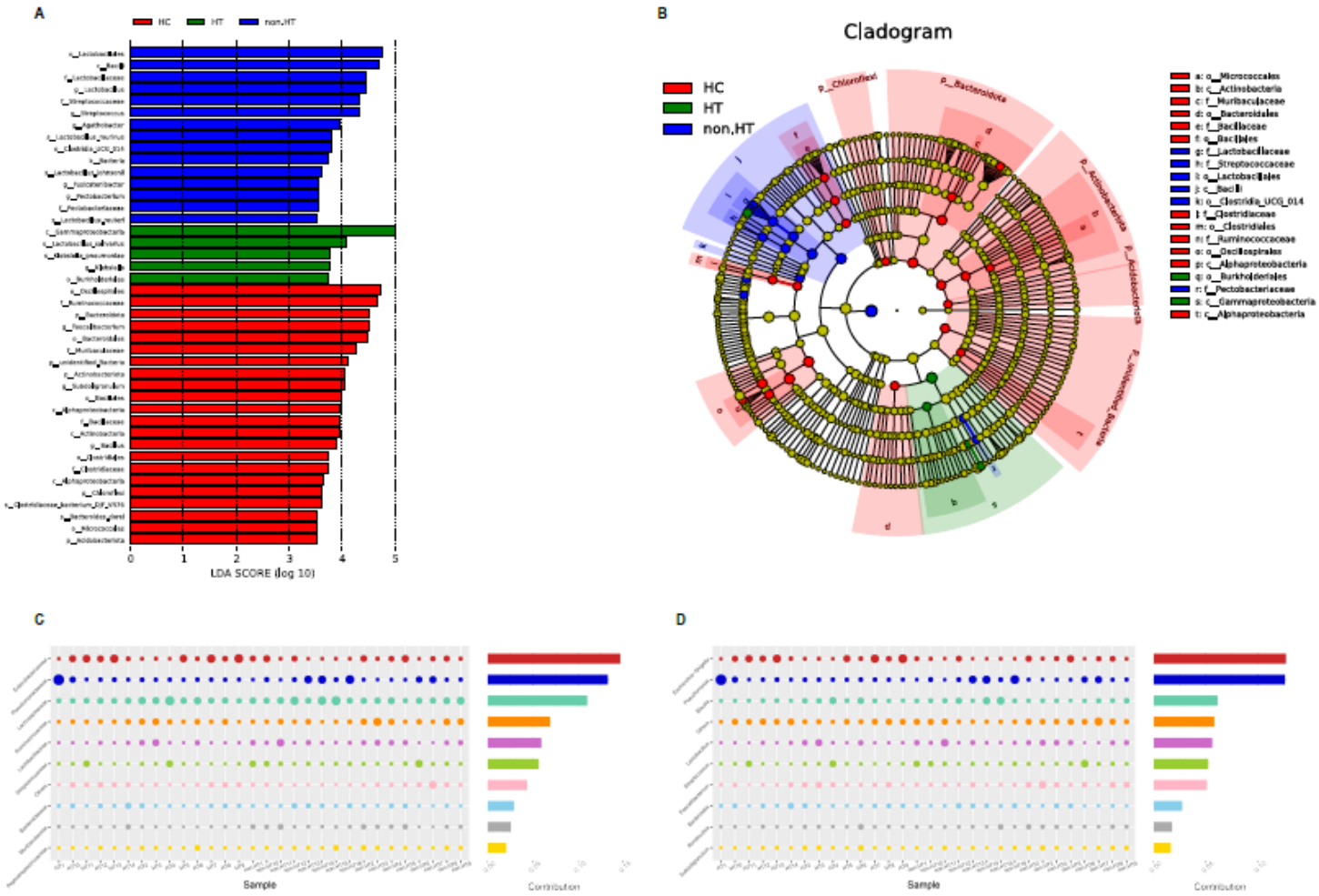

Figure 3

Predicted gut microbiome taxa linear discriminant analysis effect sizes. (A). Gut microbiome taxa that are different among healthy subjects, HT and non-HT subjects, with a linear discriminant analysis (LDA) score of least 3.5. (B). LEfSe showing bacterial taxa with significant differences in abundance among groups by cladogram. (C-D). Similarity percentage analysis (SIMPER) was performed to evaluate sample dissimilarity contribution [%] for each family (C) and genus (D) based on their relative abundance. Only families and genus with >1% dissimilarity contribution are indicated by name. Color coding of the bars indicate higher families and genus as used in HT group.

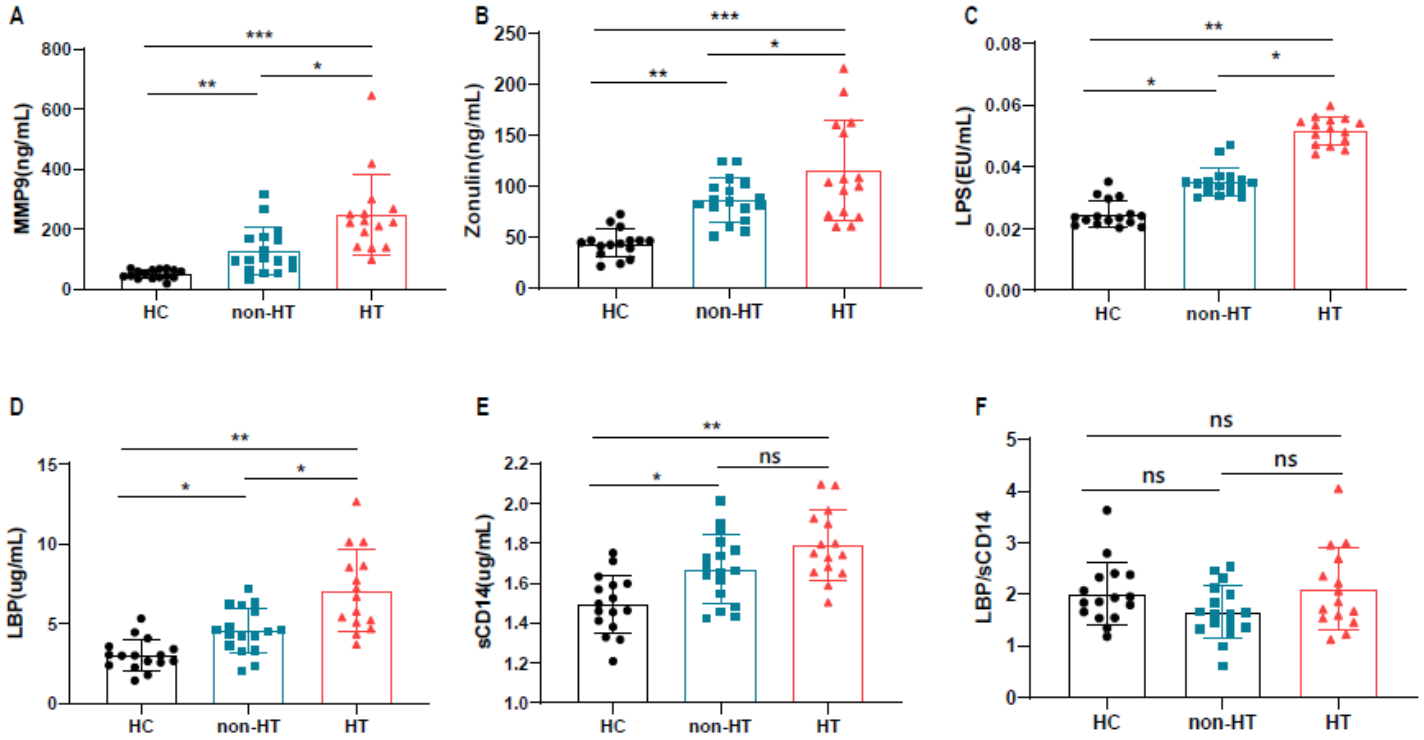

Figure 4

Plasma levels of LPS-related inflammation and barrier evaluation. (A). The blood-brain barrier permeability maker plasma MMP9 levels in different groups. (B). The intestinal barrier permeability marker plasma zonulin levels among the three groups. (C-F). plasma concentrations of LPS, LBP, sCD14, and LBP/sCD14 ratio in the three groups. n= 15-17 per group. Data are presented as mean ± SD. *P < 0.05, **P < 0.01, ***P < 0.001.

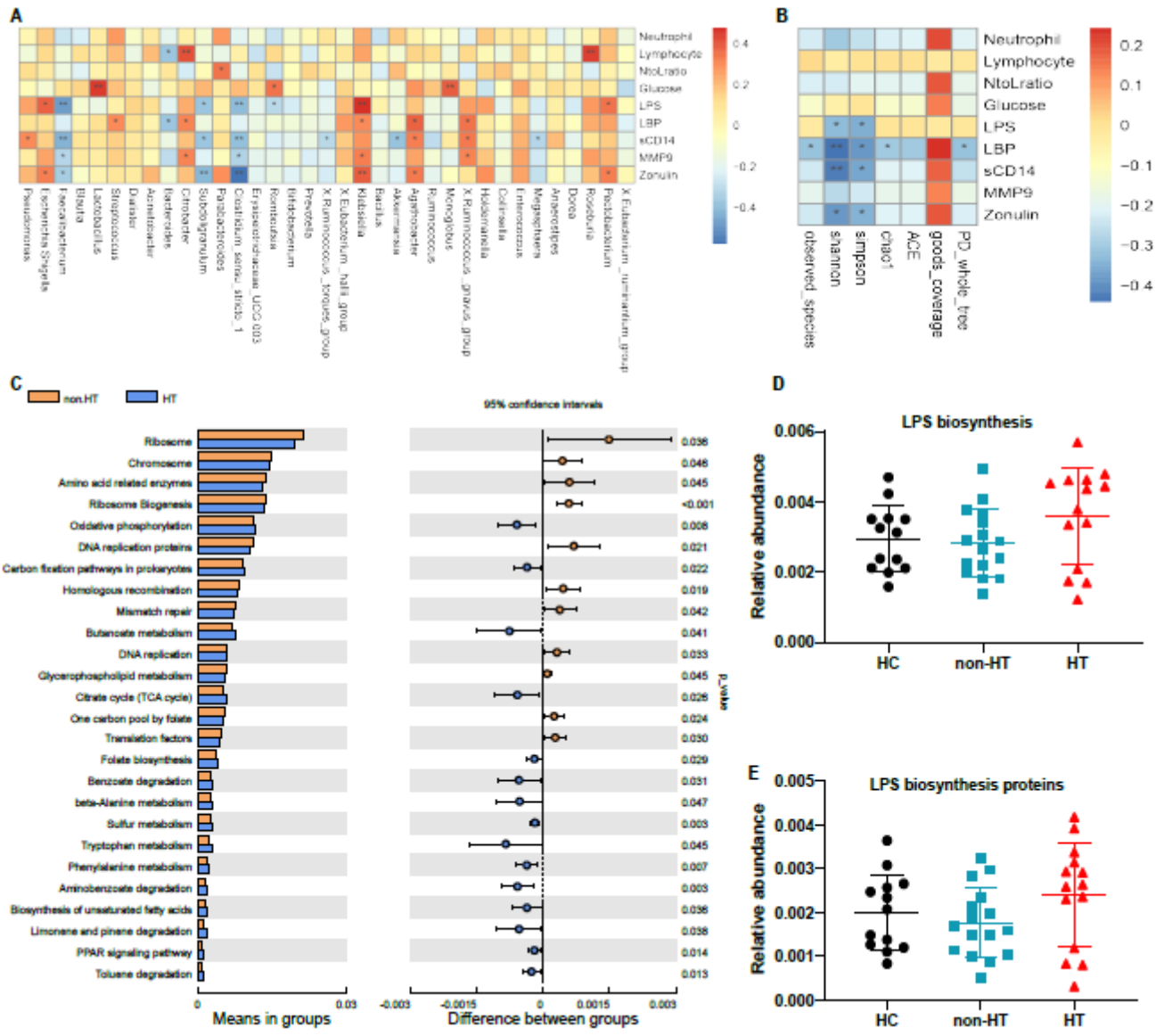

Figure 5

Gut microbial gene pathways are altered in HT. (A-B). Spearman analysis in LPS-related inflammation and barrier function correlated with bacteria (A) and alpha diversity (B). (C). The PICRUSt analysis based on KEGG database used to predict microbial metabolic function and analyze the functional differences (as detected by STAMP analysis). (D-E). Pathways relevant to LPS and LBP biosynthesis. Data according to PICRUSt server.

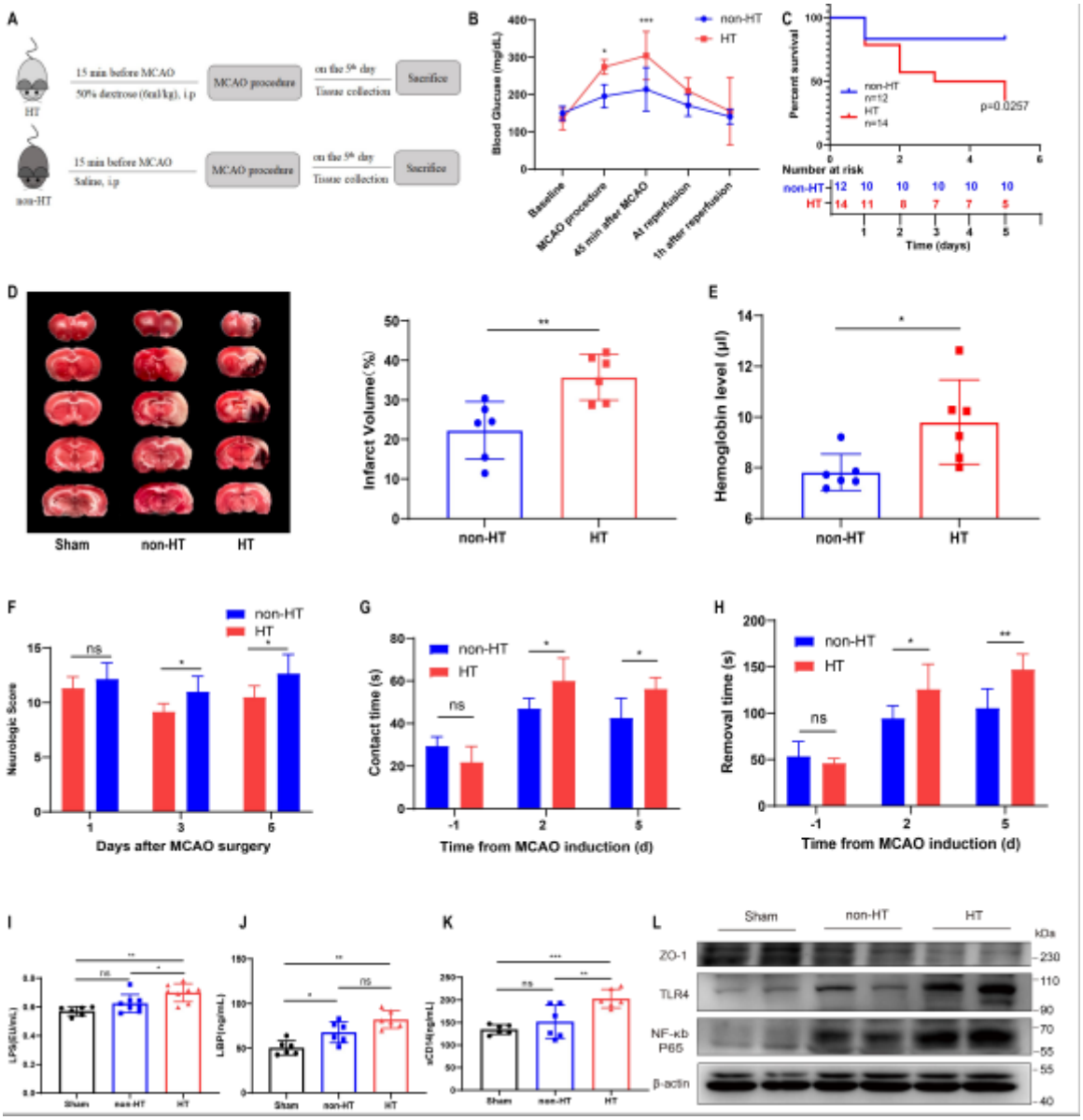

Figure 6

The key component of LPS-induced inflammation in HT model. (A). The flow chart of HT procedure. (B). Blood glucose levels through surgery in HT and non-HT group. (C). Survival curve and number at risk, log-rank test. (D). Representative photographs of brain slices with TTC stain showing the ischemic stroke and hemorrhage transformation and analysis of infarction volume in different groups. (E). The hemoglobin content in the ischemic hemisphere which is used as a measure of the severity of bleeding. (F). Neurological deficits measured by Garcia score 1, 3, and 5 d after MCAO surgery. (G and H). Sensorimotor function in HT and non-HT group. Graphs show contact time (G) and time to removal of the tape (H) from the contralateral forepaw 1 d before, and 2 d and 4 d after MCAO induction (n=6 rats per group). (I-K). Plasma levels of LPS, LBP, and sCD14 were measured in different groups. (L). The expression of ZO-1, TLR4, and phosphorated NK-κB p65 was detected by western blot in the colon. Data are presented as mean ± SD. *P < 0.05, **P < 0.01, ***P < 0.001.

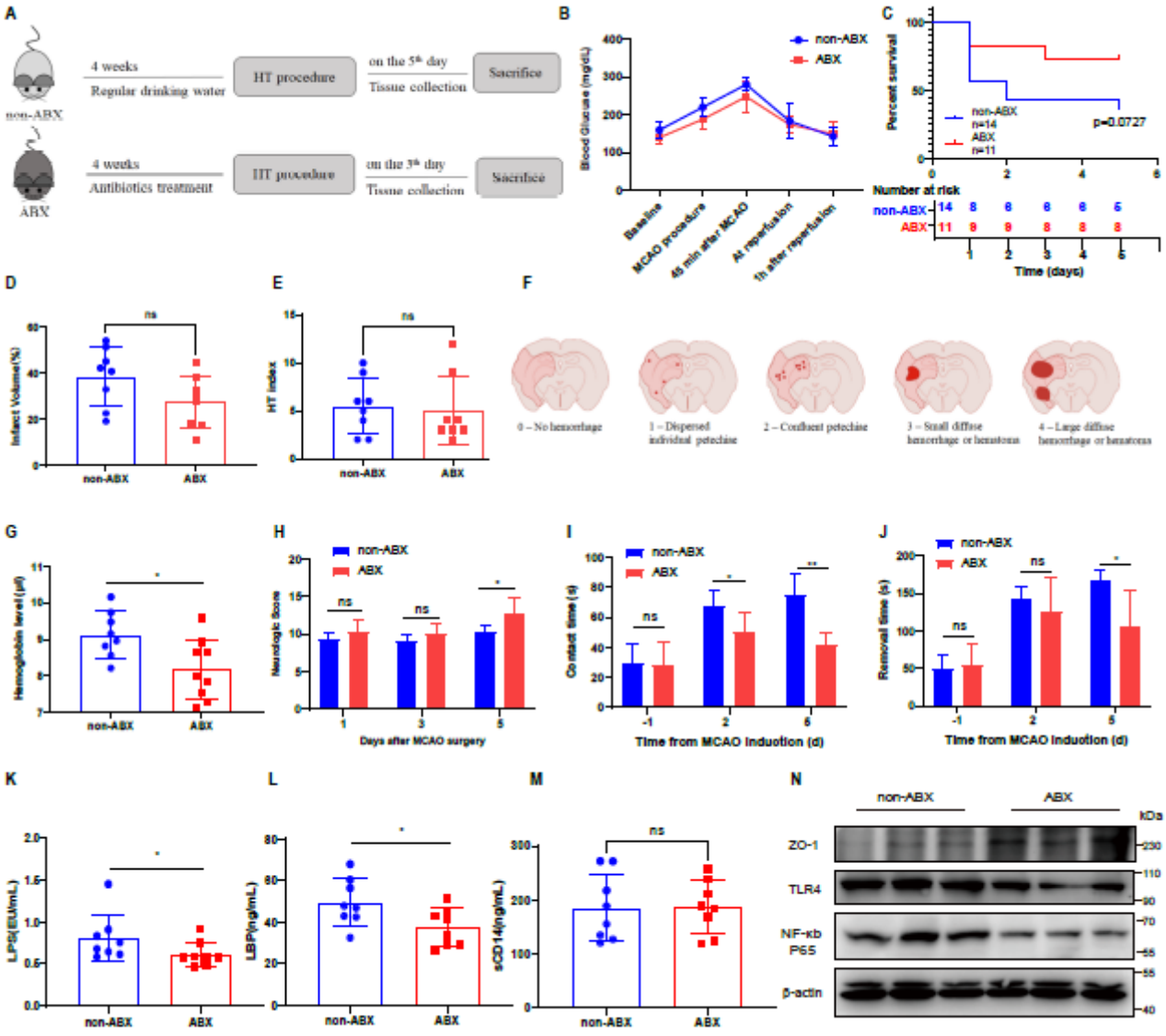

Figure 7

Antibiotics treatment alleviates LPS-induced inflammation in HT model. (A). Experimental design for antibiotics treatment. After acclimatization for 1 week, rats received antibiotics in drinking water for 4 weeks. And then the rats subjected to HT procedure. Behavior tests were measured at different time points. (B). Blood glucose levels were measured at different time points. (C). Survival curve and number at risk, log-rank test. (D). quantification of infarct volumes in ABX and non-ABX group. (E and F). Macroscopic HT assessed using HT index. (G). Hemoglobin content in ischemic hemisphere. (H). Neurologic function evaluated by Garcia score at different time points. (I and J). Adhesive removal tests 1 d before and 2 d and 4 d after MCAO induction. (K-M). The levels of LPS, LBP, and sCD14 in plasma measured by ELISA kit. (N). Expression of ZO-1, TLR4, and phosphorated NK-κB p65 proteins in the two groups measured by WB analysis. n=8 animals per group. Data are presented as mean ± SD. *P < 0.05, **P < 0.01, ***P < 0.001.

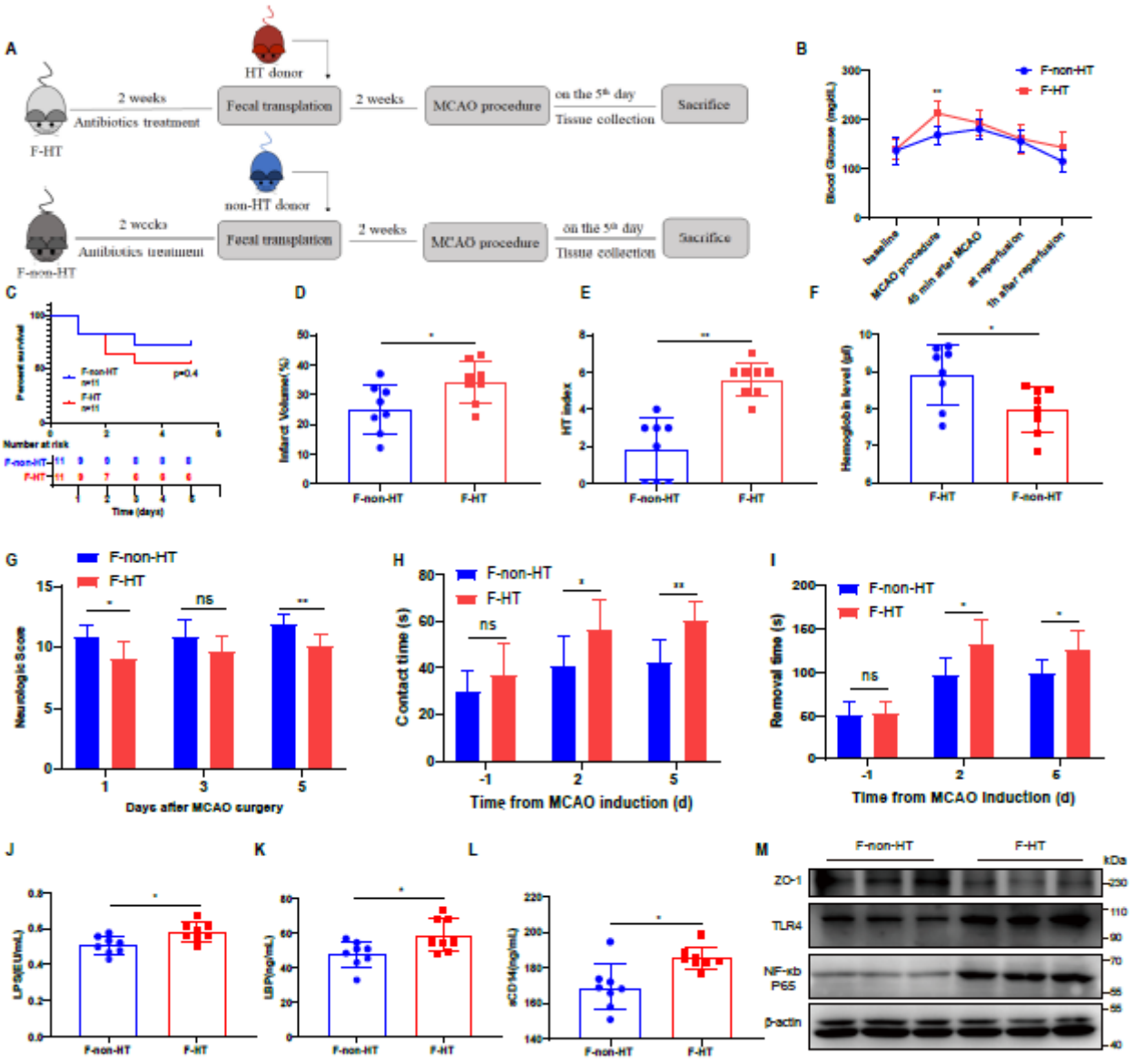

Figure 8

The changes of LPS-related signaling in recipient rats after FMT. (A). Fecal transplant experimental design. Rats were treated with antibiotics for 2 weeks and gavaged with fresh stool from either HT or non-HT donors. After 2 weeks on water, MCAO was induced in the recipient rats, and they were killed 5 d later to quantify infarct volume and hemorrhage transformation. (B). The levels of blood glucose monitored in the different groups. (C). Survival curve and number at risk. (D). percentages of the infarct volume measured in different groups. (E). Calculation of hemorrhagic score according to the classification showed in Fig. 6F. (F). Brain hemoglobin levels were evaluated 5 d after MCAO. (G-I). neurologic function evaluated by Garcia score and Adhesive removal tests. (J-L). Comparation of LPS, LBP, and sCD14 concentration in different groups. (M). Western blot analysis showing the proteins level of ZO-1, TLR4, and phosphorated NK-κB p65 proteins. Data are presented as mean ± SD. *P < 0.05, **P < 0.01, ***P < 0.001.

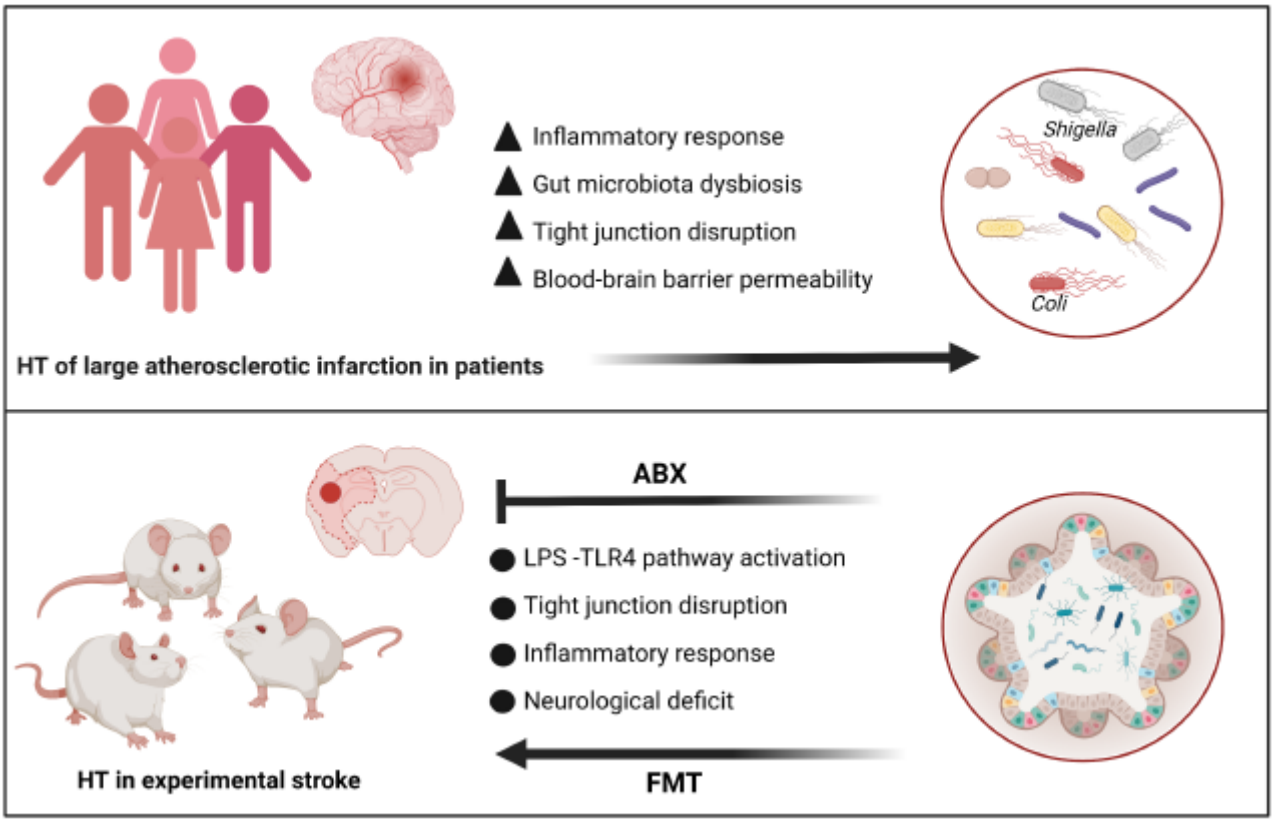

Figure 9

Schematic of the gut-microbiota-brain axis in hemorrhagic transformation. The changes of commensal bacteria in HT patients with large-artery atherosclerotic stroke is significant, especially the increased relative abundance of Escherichia–Shigella and Coli, the most origin of LPS in pathogenic microoganisms. Consistently, the key components of LPS pathway, including LPS, LBP, and sCD14 concentration, are increased in patient's plasma. The compromised function of gut and brain barrier may contribute to the systemic inflammation in HT. Furthermore, our data from a HT model in which alterations of microbiota induced by antibiotics treatment and fecal transformation influence LPS-induced inflammation and stroke outcomes, which may be due to activation of TLR4 signaling, and subsequently regulate HT progress.

Supplementary Files

This is a list of supplementary files associated with this preprint. Click to download.

- Supplementarymaterial.docx
- Fig.s1.pdf
- Fig.s2.pdf